

Primordial black holes from single field models of inflation

Juan García-Bellido,^a Ester Ruiz Morales^b

^aInstituto de Física Teórica UAM-CSIC, Universidad Autónoma de Madrid, Cantoblanco, 28049 Madrid, Spain

^bDepartamento de Física, ETSIDI, Universidad Politécnica de Madrid, 28012 Madrid, Spain

Abstract. Primordial black holes (PBH) have been shown to arise from high peaks in the matter power spectra of multi-field models of inflation. Here we show, with a simple toy model, that it is also possible to generate a peak in the curvature power spectrum of single-field inflation. We assume that the effective dynamics of the inflaton field presents a near-inflection point which slows down the field right before the end of inflation and gives rise to a prominent spike in the fluctuation power spectrum at scales much smaller than those probed by Cosmic Microwave Background (CMB) and Large Scale Structure (LSS) observations. This peak will give rise, upon reentry during the radiation era, to PBH via gravitational collapse. The mass and abundance of these PBH is such that they could constitute the totality of the Dark Matter today. We satisfy all CMB and LSS constraints and predict a very broad range of PBH masses. Some of these PBH are light enough that they will evaporate before structure formation, leaving behind a large curvature fluctuation on small scales. This broad mass distribution of PBH as Dark Matter will be tested in the future by AdvLIGO and LISA interferometers.

Contents

1	Introduction	1
2	Single-field toy model of inflation	3
2.1	Slow-roll parameters and Number of e-folds	5
3	Power spectrum from single field inflation	7
3.1	$P_R(k)$ at large scales: CMB and LSS	8
3.2	$P_R(k)$ at small scales: PBH	9
4	Production of Primordial Black Holes	10
4.1	PBH evaporation in broad mass distributions	11
5	Discussion and Conclusions	12

1 Introduction

The nature of Dark Matter (DM) is one of the remaining mysteries of Modern Cosmology. We know it exists since at least 1933, from the first observations of galaxy cluster dynamics by Fritz Zwicky, all the way to full consistency with CMB anisotropies observed by Planck, and LSS formation measured by galaxy surveys. For a recent review see [1]. Its nature is still unknown. There are more than forty orders of magnitude in mass for the range of possible fundamental constituents, from ultralight axions [2] to supermassive black holes [3, 4]. Some of the possible Particle Dark Matter (PDM) candidates have recently been strongly constrained as the dominant component of DM (e.g. massive neutrinos, WIMPS, heavy axions, etc.), although there is still room for more exotic components.

In this paper we assume that DM is composed primarily of Primordial Black Holes. The first time a connection between PBH and DM was made was in the paper of Chapline [5], where the lightmass PBH of Carr and Hawking [6] were supposed to constitute part of the DM. Later on, in 1993, Dolgov and Silk [7] suggested a model of matter fluctuations which used the QCD transition as a trigger for the formation of PBHs of order a solar mass, which was later developed by Jedamzik [8]. These papers relied on the first order nature of the QCD transition to amplify the minute matter fluctuations produced during inflation into high density regions that would gravitationally collapse to form the PBH. We know nowadays that the QCD transition is not first order but a crossover [9], so such a mechanism is ruled out.

An alternative is to produce a large peak in the curvature power spectrum which would collapse to form black holes even without a phase transition. The first time such a peak was used to generate PBH as the main component of DM was proposed by García-Bellido, Linde and Wands in 1996, based on a two-field hybrid model of inflation [10]. Soon afterwards, many papers appeared in the literature making use of such peaks in the spectrum [11, 12] to generate a whole range of masses for PBHs as the main constituent of DM. Broad peaks arise from quantum fluctuations of the inflaton field that backreact on the metric and induce large curvature perturbations [13]. When those fluctuations re-enter the horizon during the radiation era, their gradients induce a gravitational collapse that cannot be overcome even by the radiation pressure of the expanding plasma, producing black holes with a mass of order

the horizon mass [10]. Most of these PBH survive until today, and dominate the universe expansion at matter-radiation equality.

Other models of PBH production via peaks in the matter power spectrum have been proposed in the literature, see e.g. [14]. They all assume a model of inflation with multiple fields. One of the fields acts like the inflaton and the other one either triggers a phase transition or an explosive productions of gauge particles or a fast evolution, all of which backreact on the curvature generating a peak in the spectrum of curvature fluctuations. Depending on when does this phenomenon occur during inflation, i.e. how many e-folds before the end of inflation, we may have a narrow or a broad spectrum of masses for the PBHs that form during the radiation era upon re-entry. It is relatively easy in these models to separate the large scale fluctuations we observe in the CMB and LSS, that correspond to $N = 65 - 55$ e-folds, from the small scale fluctuations responsible for PBHs, corresponding to $N \sim 40 - 20$ e-folds before the end of inflation.

In this paper we explore single-field models of inflation that may give rise to peaks in the curvature power spectrum responsible for the formation of PBHs. In the absence of a second field that triggers the growth of fluctuations, like in hybrid inflation [13], we need a period of evolution during inflation where a single field (the inflaton) slows down, creating a stronger backreaction and a quick growth in curvature fluctuations. In terms of dynamics, this effect can only be achieved by producing a plateau in the inflationary potential, which slow-rolls the inflaton even further than usual, before ending inflation. The best way to produce this plateau is with an inflection point in the potential. The problem, in this case, is that the inflaton may stay too long at the inflection point, diluting away the inflationary fluctuations that had successfully imprinted the metric on large scales to explain the CMB anisotropies.

We have succeeded within single-field inflation to generate a large peak in the matter power spectrum at small scales by introducing in the potential a near-inflection point. The toy-model we propose has the minimum number of parameters needed to produce the peak without fine-tuning. The main feature of this type of model is that the peak is very broad, and covers many orders of magnitude in mass. In order to account for DM it requires a small fraction $f_{\text{PBH}}(M)$ of the total Ω_M at any given mass interval. This may be the reason why they have not yet been detected by microlensing events or other phenomena that put severe bounds on them. On the other hand, since the peak is broad, it may affect the rate of structure formation since recombination, generating heavy seeds on which supermassive black holes may grow by gas accretion to become the beacons we observe as quasars at high redshift, emitting in X-rays [15, 16] and starting early reionization [17].

With the advent of Gravitational Wave Astronomy, we have a completely new window into the Early Universe. The fact that PBH are formed in clusters in this scenario [13], see also [18, 19], makes them more prone to merging within the age of the universe, and binary inspirals are expected at a higher rate than if they were uniformly distributed in space. For this reason, Clesse and García-Bellido predicted in 2015 [13] that LIGO would be able to detect the final merging of massive BH binaries (BHB), as it actually occurred a few months later [20]. The large masses of the progenitors (36 and 29 solar masses) prompted the attention of the community, which immediately suggested a connection between Dark Matter and PBH [21–23], and initiated a search for a variety of formation mechanisms to be explored, including both primordial [3, 14, 24–28] and via stellar evolution [29, 30]. A few months later we learned that there had been three BHB merger events in LIGO Run O1 [31–33]. Furthermore, last week the LIGO collaboration announced two more events. The surprisingly high rate of merger events suggests that black holes are more abundant and

more clustered than expected, in agreement with the PBH scenario.

Moreover, not only do we have individual BHB merger events, but soon we will be able to detect the Stochastic GW Background from such inspirals in LIGO [34], happening all the way from recombination until today, if they arise from PBHs [35, 36]. Moreover, in the near future, the space interferometer LISA should have this as a new irreducible background [37], and will be able to measure the main parameters of the PBH mass distribution.

The paper is structured as follows. In Section 2 we introduce the single-field toy model of inflation and obtain an exact expression for the number of e-folds of inflation. In Section 3 we compute the curvature power spectrum for this simple model at all scales, comparing the amplitude at large scales (CMB and LSS) with that at small scales (responsible for PBH). In Section 4 we study the production of PBH and their evaporation, and we conclude with an overall discussion of the scenario in Section 5.

2 Single-field toy model of inflation

Although several multi-field models of inflation have been proposed that give rise to peaks in the matter power spectrum, e.g. by having a mild waterfall regime at the transition between slow-roll and the symmetry breaking stage of hybrid inflation [13], no compelling single-field model of inflation exists that can give a significant spike in the matter power spectrum of fluctuations.

In this paper we show that a single-field scalar potential with a near-inflection point can also give rise to a peak in the matter power spectrum. This simple and quite generic feature of the potential makes the inflaton enter into an ultra-slow-rolling stage during a short range of e-folds that generates the spike in the spectrum. One has to be careful however that this new feature in the potential does not affect the already constrained spectrum on CMB and LSS scales. In multi-field models like hybrid inflation this can easily be achieved, since one can decouple the two stages (CMB and PBH) by the intermediate waterfall stage, which arises due to the coupling to the symmetry breaking field. As we will see, in single field models of inflation, those two stages are intimately related, imposing much tighter constraints on the model parameters.

We propose a single-field toy model constructed as a ratio of polynomials, in order to take advantage of the asymptotic flatness of the potential for large values of the field, which seems to be in agreement with CMB observations. Rather than starting below (but close to) the inflection point, as usually done in MSSM inflation [38, 39], in Accidental Inflation [40] and in more general Inflection-point Inflation [41], we will assume that the field starts at larger values, well above the inflection point, and then slow-rolls down towards the minimum of the potential, crossing the near-inflection point a few (typically 30 to 40) e-folds before the end of inflation.

The inflationary potential we propose as toy-model is given by

$$V(\phi) = \left(\frac{1}{2} m^2 \phi^2 - \frac{1}{3} \alpha v \phi^3 + \frac{1}{4} \lambda \phi^4 \right) \left(1 + \xi \phi^2 \right)^{-2}, \quad (2.1)$$

which can be recast in the form

$$V(x) = \frac{\lambda v^4}{12} \frac{x^2(6 - 4ax + 3x^2)}{(1 + bx^2)^2}, \quad (2.2)$$

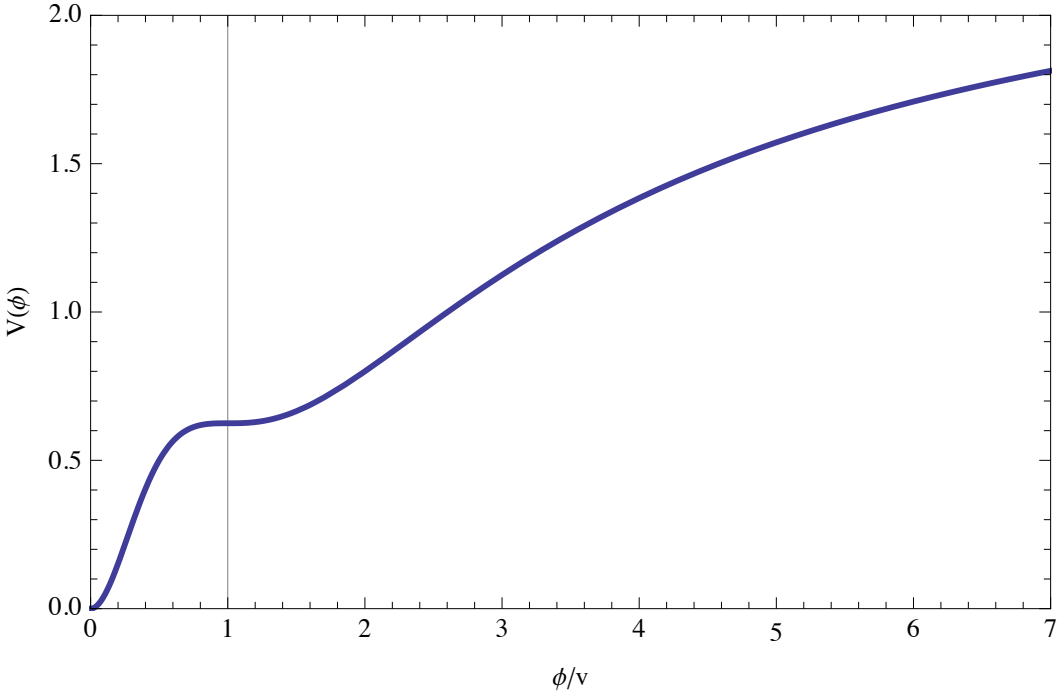


Figure 1. Single field potential $V(\phi)$ (in arbitrary units) with an inflection point (vertical line) and an asymptotically flat plateau. The parameters chosen are $a = 3/2$ and $b = 1$, which give an inflection point at $\phi = v$.

under a redefinition of parameters, $x = \phi/v$, $m^2 = \lambda v^2$, $a = \alpha/\lambda$ and $b = \xi v^2$. Although there are four independent parameters (m , α , λ , ξ), we can see that only two of them are relevant for the evolution during inflation near the inflection point, i.e. (a, b) . We have plotted in Fig. 1 the potential, for specific values of the parameters, which shows an inflection point at small values of the field.

This potential has an inflection point, $V'(\phi) = V''(\phi) = 0$, for certain values of the parameters (a, b) which can be obtained by solving the third order equation

$$1 - a x + (1 - b) x^2 + \frac{ab}{3} x^3 = 0, \quad (2.3)$$

The three solutions of Eq. (2.3) are given by $x = x_1 < 0$ and $x_{2,3} = x_0 \pm i y_0$, with

$$x_1 = \frac{b-1}{ab} - \frac{1}{ab} \left(\Theta(a, b) + \frac{(b-1)^2 + a^2 b}{\Theta(a, b)} \right), \quad (2.4)$$

$$x_0 = \text{Re } x_2 = \frac{b-1}{ab} + \frac{1}{2ab} \left(\Theta(a, b) + \frac{(b-1)^2 + a^2 b}{\Theta(a, b)} \right), \quad (2.5)$$

$$y_0 = \text{Im } x_2 = \frac{\sqrt{3}}{2ab} \left(\Theta(a, b) - \frac{(b-1)^2 + a^2 b}{\Theta(a, b)} \right), \quad (2.6)$$

and

$$\Theta(a, b) = \left(\sqrt{3} ab \sqrt{\Delta(a)^3 - \left(b - 1 + \frac{1}{3} a^2 \right)^3} + (1 - b)^3 + \frac{3}{2} a^2 b \right)^{1/3}. \quad (2.7)$$

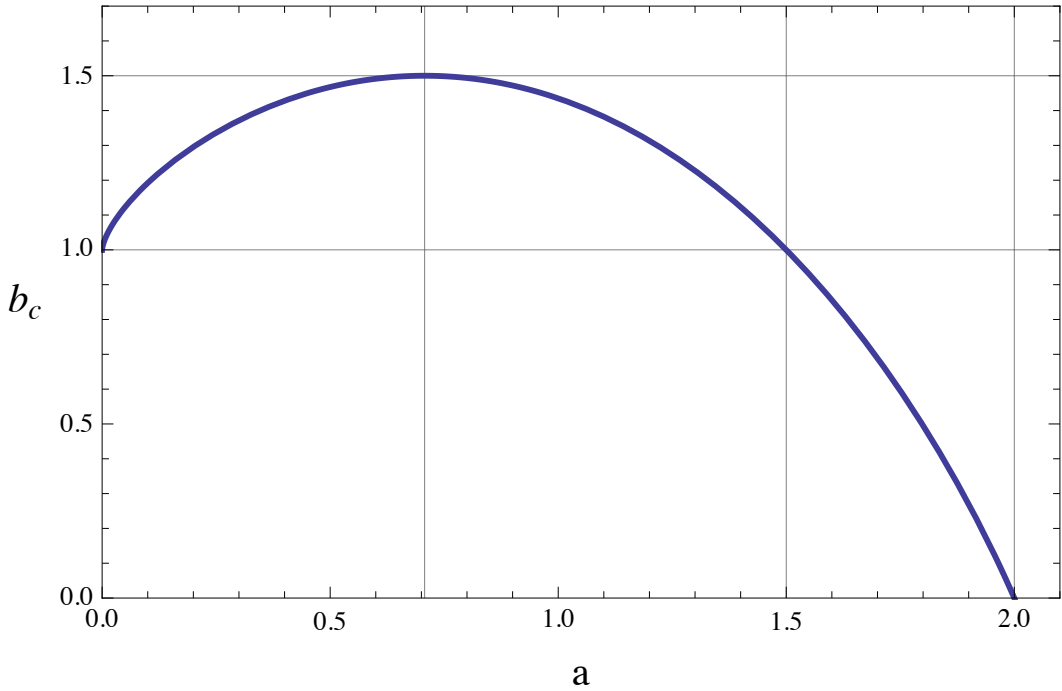


Figure 2. The critical values of the model parameter b for which there are inflection points in the potential (2.2) as a function of a .

The potential will have inflection points at real values of x (one negative and two real, identical and positive) whenever the parameter b acquires a critical value (as a function of a)

$$b_c(a) = 1 - \frac{1}{3} a^2 + \Delta(a), \quad (2.8)$$

$$\Delta(a) = \frac{a^2}{3} \left(\frac{9}{2a^2} - 1 \right)^{2/3}. \quad (2.9)$$

We have plotted the critical values b_c as a function of a in Fig. 2. Note that there is a maximum value of b_c and also a maximum value of a for which the critical b parameter is positive.

For these critical values, the solutions of the cubic equation simplify to

$$x_1 = \frac{b_c - 1 - 2\sqrt{(b_c - 1)^2 + a^2 b_c}}{a b_c} < 0, \quad (2.10)$$

$$x_2 = x_3 = \frac{b_c - 1 + \sqrt{(b_c - 1)^2 + a^2 b_c}}{a b_c} > 0. \quad (2.11)$$

2.1 Slow-roll parameters and Number of e-folds

In this type of potential the slow-roll parameter ϵ can be calculated exactly

$$\epsilon = \frac{1}{2\kappa^2} \left(\frac{V'(\phi)}{V(\phi)} \right)^2 = \frac{8}{\kappa^2 v^2} \frac{(3 - 3 a x + 3(1 - b)x^2 + a b x^3)^2}{x^2 (6 - 4 a x + 3 x^2)^2 (1 + b x^2)^2}, \quad (2.12)$$

and the number of e-folds is given by

$$N = \int \frac{\kappa d\phi}{\sqrt{2\epsilon}} = \frac{\kappa^2 v^2}{4 a b} \int \frac{x (6 - 4 a x + 3 x^2) (1 + b x^2)}{(x - x_1) ((x - x_0)^2 + y_0^2)} dx, \quad (2.13)$$

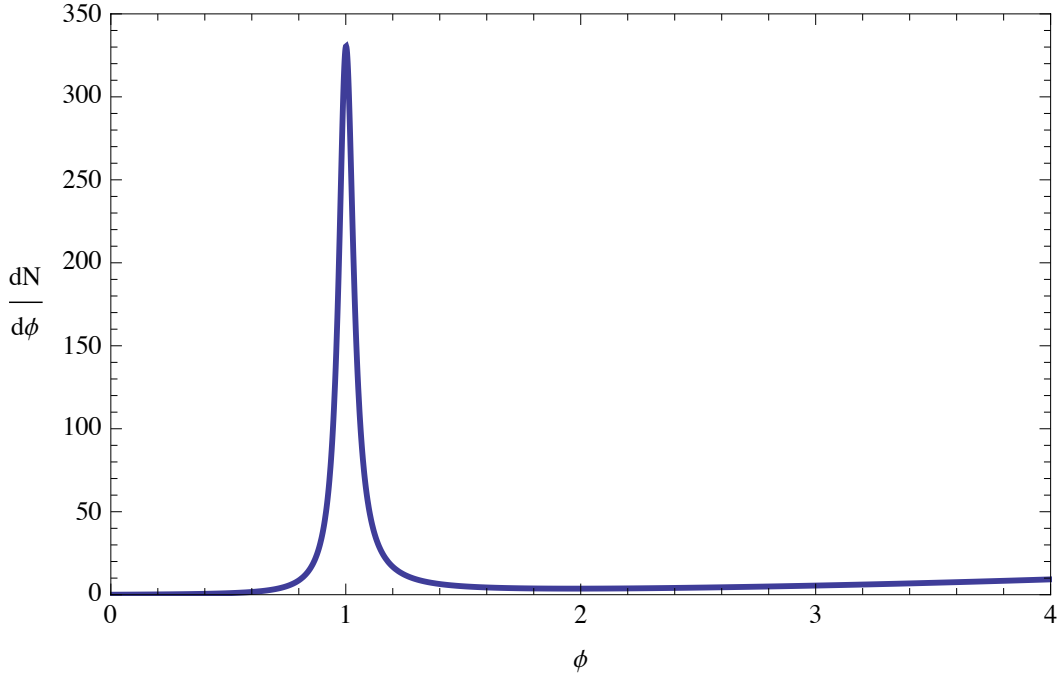


Figure 3. The integrand of the number of e-folds as a function of the field values (in units of v). The parameters chosen are $a = 3/2$ and $b = 1$, which give an inflection point at $\phi = v$. We have chosen the resonance parameter $\beta = 0.002$. The area under the curve will give the number of e-folds spent close to the resonance.

which can be integrated and gives the following leading terms

$$N = \frac{\kappa^2 v^2}{4a} \left[x^3 + x^2 \frac{9(b-1) - 4a^2 b}{2ab} + x \frac{(108 \Delta[a])^{3/4}}{ab^2} + \frac{f(a, b)}{y_0 ((x - x_0)^2 + y_0^2)} \left(\arctan \left(\frac{x - x_0}{y_0} \right) + \arctan \left(\frac{x_0}{y_0} \right) \right) \right]. \quad (2.14)$$

Clearly, for (a, b) in their critical values, $y_0 \rightarrow 0$ and N diverges when the inflaton passes through the inflection point. Therefore, we cannot chose parameters (a, b) to give an *exact* inflection point in the potential, but the values can be sufficiently close to the critical values to generate a near-inflection point. In that case, we can have a large number of e-folds spent at $x = x_0$ to produce a significant peak in the matter power spectrum, and yet have a sufficiently flat region of the potential around $N = 65$ in order to generate the correct CMB anisotropies. We have plotted the integrand of Eq. (2.13) in Fig. 3 to show the Breit-Wigner shape of the resonance at $x = x_0$ for a near-inflection point. The area under the curve will give the number of e-folds spent close to the resonance. This tremendous peak will be responsible for a slow-down of the field and a corresponding large spike in the matter power spectrum.

For values of (a, b) very close to the critical ones, we have the resonance parameter $\beta \equiv b_c(a) - b \ll 1$, and the solutions x_1 and x_0 are given by Eqs. (2.10) and (2.11) respectively,

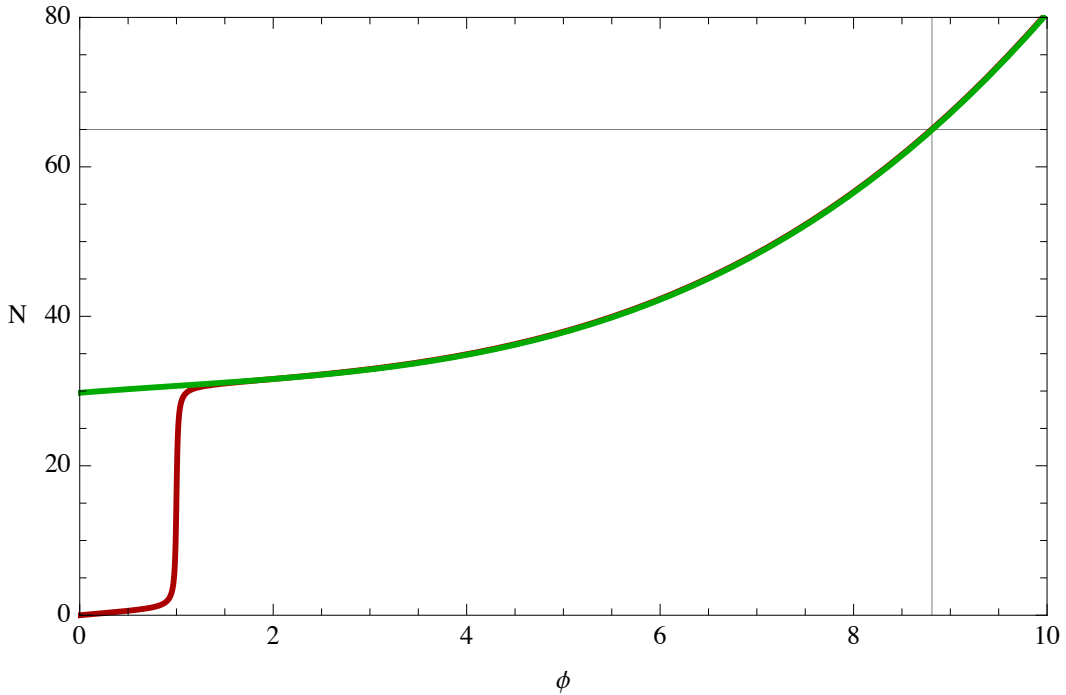


Figure 4. The number of e-folds N of inflation (2.13) for a typical model with a near-inflection point (red line) as a function of the field values in units of v . The parameters chosen are $a = 3/2$ and $b = 1$, which give an inflection point at $\phi = v$. We have chosen the resonance parameter $\beta = 0.002$ and $\Delta N = 30$. We also compare here with the upper branch approximation (in green), see Eq. (2.16).

while y_0 can be approximated, to lowest order in β , by

$$y_0 = \frac{\sqrt{3} \Delta(a)}{(b_c - 1)^2 + a^2 b_c} \sqrt{\beta}. \quad (2.15)$$

In this regime of near-inflection point, the number of e-folds jumps at $x = x_0$ by a large factor ΔN and the number of e-folds in the upper branch region can be extremely well approximated by

$$N_* = \frac{\kappa^2 v^2}{4a} x^3 + \Delta N, \quad (2.16)$$

$$\Delta N = \frac{3\pi}{2} \frac{\kappa^2 v^2}{a^{7/4}} \frac{(3/\sqrt{2} - a)^{1/2}}{\sqrt{\beta}}. \quad (2.17)$$

It is clear from this expression that the shift ΔN is inversely proportional to $\sqrt{\beta}$, as expected. The closer we are to the critical value of b giving rise to the point of inflection, the larger the number of e-folds spent at the critical point. In Fig. 4 we show that this approximate solution (2.16) fits very well the exact number of e-folds (2.13) for values of the inflaton field above the inflection point.

3 Power spectrum from single field inflation

In this section we compute the curvature power spectrum and make sure that a peak at small scales will not conflict with the good properties of the spectrum at CMB and LSS scales.

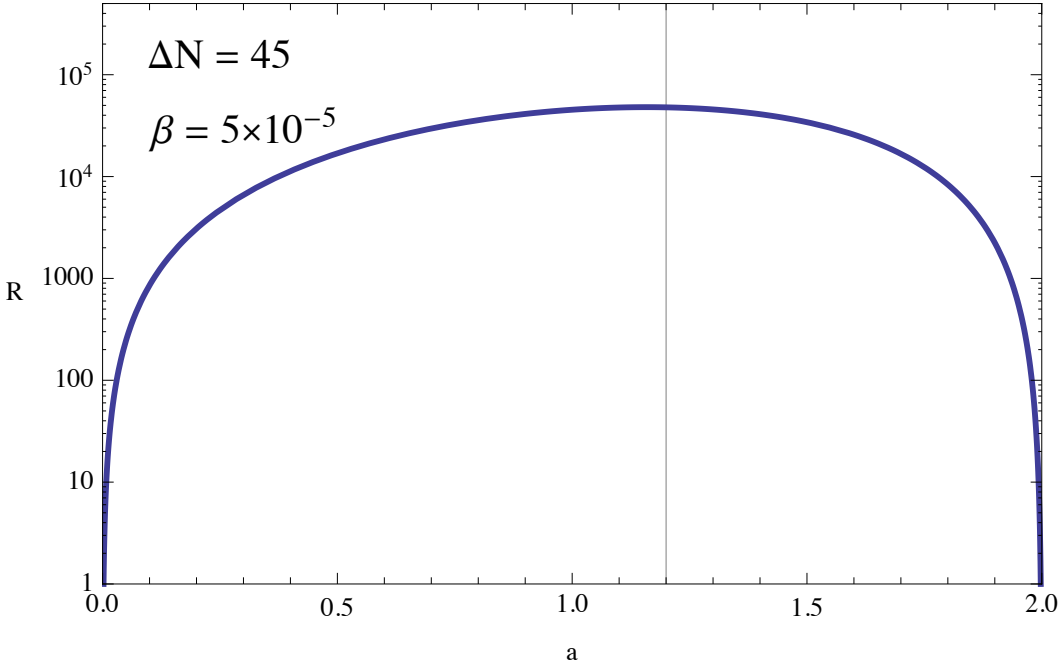


Figure 5. The ratio of the power spectrum at the resonant peak versus the amplitude at CMB scales as a function of the inflection point parameter a , for a choice of ΔN and β .

The power spectrum is related to the potential (2.2) and the slow-roll parameter (2.12) by

$$P_{\mathcal{R}}(k) = \frac{\kappa^2}{2\epsilon} \left(\frac{H}{2\pi} \right)^2 = \frac{\kappa^4 V(x)}{24\pi^2 \epsilon(x)} = \frac{\lambda \kappa^6 v^6}{96 \times 24\pi^2} \frac{(6 - 4a x + 3x^2)^3 x^4}{a^2 b^2 (x - x_1)^2 ((x - x_0)^2 + y_0^2)^2}, \quad (3.1)$$

as a function of the inflaton field value x (in units of v), parametrically dependent on scale k via the number of e-folds $N(x)$ through Eq. (2.14).

It is convenient to study the behavior of the power spectrum at different asymptotic regimes in order to easily check its compatibility with existing CMB and LSS bounds and the amount of PHB produced at low scales.

3.1 $P_{\mathcal{R}}(k)$ at large scales: CMB and LSS

The power spectrum at scales corresponding to the CMB, i.e. for large inflaton values ($x_{65} \gg x_0$), is approximately given by

$$A_s^2 = P_{\mathcal{R}}(x_{65}) \simeq \frac{\lambda \kappa^6 v^6}{96 \times 24\pi^2} \frac{27 x_{65}^4}{a^2 b^2}, \quad (3.2)$$

where x_{65} is the inflaton value 65 e-folds before the end of inflation (in units of v). Note that for those large values the number of e-folds, the exact value of N given in (2.13) is extremely well approximated by N_* in (2.16), while the slow-roll parameter asymptotically behaves like

$$\epsilon_* \simeq \frac{8 a^2}{9 \kappa^2 v^2 x^4} \simeq \frac{(2 \kappa^2 v^2 a^2)^{1/3}}{9(N_* - \Delta N)^{4/3}}. \quad (3.3)$$

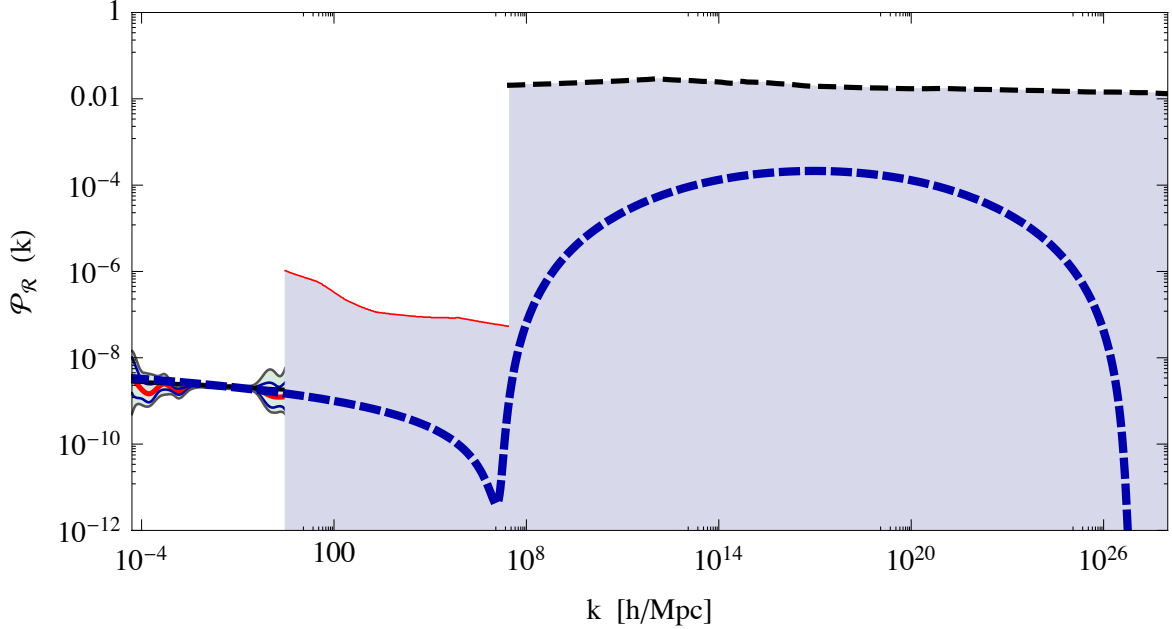


Figure 6. The matter power spectrum, for model parameters: $a = 3/2$, $b = 1$, $\Delta N = 45$ and $\beta = 5 \times 10^{-5}$. We have also plotted the range of values allowed by Planck (2015), by compact minihalos (red line) and by PBH (black dashed line), at 95% c.l. (Figure adapted from Ref. [43]).

Computing from here the scalar spectral index, we find [42]

$$n_s = 1 - 2\epsilon(N) + \frac{\epsilon'(N)}{\epsilon(N)} \simeq 1 - \frac{2(2\kappa^2 v^2 a^2)^{1/3}}{9(N - \Delta N)^{4/3}} - \frac{4}{3(N - \Delta N)}. \quad (3.4)$$

There is a whole range of parameters that satisfy the Planck constraints [44, 45], i.e. that give the right amplitude, $\ln(10^{10} A_s^2) = 3.094 \pm 0.068$, the spectral index, $n_s = 0.9645 \pm 0.0098$, the running of the spectral index, $dn_s/d\ln k = -0.0065 \pm 0.0152$, and the proper bound on the tensor to scalar ratio, $r < 0.09$ at 95 % c.l., for modes that left the horizon 65 e-folds before the end of inflation, corresponding to our horizon today. We have chosen a particular set of values, $a = 3/2$, $b = 1$, $\Delta N = 45$ and $\beta = 5 \times 10^{-5}$, that satisfy the observational constraints in the whole range of scales, as can be seen in Fig. 6.

3.2 $P_R(k)$ at small scales: PBH

The power spectrum (3.1) at the scale of the near-inflection point ($x = x_0$) becomes

$$P_R(x_0) = \frac{\lambda \kappa^6 v^6}{96 \times 24\pi^2} \frac{(6 - 4a x_0 + 3x_0^2)^3 x_0^4}{9((b_c - 1)^2 + a^2 b_c) y_0^4} \quad (3.5)$$

$$= \frac{\lambda \kappa^6 v^6}{96 \times 24\pi^2} \frac{(6 - 4a x_0 + 3x_0^2)^3}{(1 - 9/(2a^2))^{8/3}} \frac{((b_c - 1)^2 + a^2 b_c)^3 x_0^4}{a^8 \beta^2}, \quad (3.6)$$

where we have used y_0 from Eq. (2.15) and the solutions x_1 and x_0 given in Eqs. (2.10) and (2.11), valid for $\beta \ll 1$. This value of $P_R(x_0)$ corresponds to the plateau in Fig. 6, valid for

a large range of e-folds ΔN around the near-inflection point. With the previous expressions we can compute the ratio between both amplitudes

$$R \equiv \frac{P_{\mathcal{R}}(x_0)}{P_{\mathcal{R}}(x_{65})} = \frac{(6 - 4a x_0 + 3x_0^2)^3}{(1 - 9/(2a^2))^{8/3}} \frac{b_c^2 ((b_c - 1)^2 + a^2 b_c)^3}{27 a^6 \beta^2} \frac{x_0^4}{x_{65}^4} \equiv R(a) \left(\frac{\Delta N}{\beta} \right)^{4/3}. \quad (3.7)$$

We have shown in Fig. 5 the dependence of this ratio on the parameter a , for a standard choice of $\Delta N = 45$ and $\beta = 5 \times 10^{-5}$. Note that significantly large ratios can easily be obtained for sharp resonances ($\beta \ll 1$).

For our choice of parameters, $\Delta N = 45$, $\beta = 5 \times 10^{-5}$, $a = 3/2$ and $b_c = 1$, we find the amplitude of the matter power spectrum at $k = 0.05 h/\text{Mpc}$ in agreement with Planck [44, 45] (i.e. $A_s^2 = 2.14 \times 10^{-9}$) for the model parameters $\lambda = 1.1 \times 10^{-7}$, and $\kappa^2 v^2 = 0.11$, which are very natural values indeed. For these values, the scalar spectral index, $n_s = 0.951$, and its running, $dn_s/d\ln k = -0.004$, are well within the Planck 95% c.l. regions, and the tensor to scalar ratio is well within limits, $r_{0.05} = 16 \epsilon_{60} = 0.03$, for prompt detection at future CMB experiments. Moreover, since the mass of the inflaton at the minimum of the potential is relatively high, $m = v\sqrt{\lambda} = 5 \times 10^{14} \text{ GeV}$, and the energy density at the end of inflation is $\rho_{\text{end}} = \frac{3}{2}V_{\text{end}} = 1.3 \times 10^{-10} M_P^4$, we expect a relatively high reheating temperature.

4 Production of Primordial Black Holes

Here we study how the peak in the matter power spectrum generates a peak in the mass distribution of black holes and how to compute their abundance as a fraction of the total Ω_M .

Assuming that the probability distribution of density perturbations are Gaussian, one can evaluate the fraction β^{form} of the universe collapsing into primordial black holes of mass M at the time of formation t_M as [13]

$$\beta^{\text{form}}(M) \equiv \left. \frac{\rho_{\text{PBH}}(M)}{\rho_{\text{tot}}} \right|_{t=t_M} = \int_{\zeta_c}^{\infty} \frac{d\zeta}{\sqrt{2\pi}\sigma} e^{-\frac{\zeta^2}{2\sigma^2}} = \frac{1}{2} \text{erfc} \left(\frac{\zeta_c}{\sqrt{2}\sigma} \right). \quad (4.1)$$

In the limit where $\sigma \ll \zeta_c$, one gets

$$\beta^{\text{form}}(M) = \frac{\sigma}{\sqrt{2\pi}\zeta_c} e^{-\frac{\zeta_c^2}{2\sigma^2}}. \quad (4.2)$$

The variance of the curvature perturbations σ is related to the power spectrum through $\langle \zeta^2 \rangle = \sigma^2 = \mathcal{P}_\zeta(k_M)$, where k_M is the wavenumber of the mode re-entering inside the Hubble radius at time t_M . If σ is above a certain threshold, $\zeta_c \simeq 0.086$, then the probability of collapse to form a PBH can be large. The mass of the PBH at formation is then given by

$$M_{\text{PBH}} = \gamma \frac{4\pi M_P^2}{H_N} e^{2N}, \quad (4.3)$$

where $\gamma \sim 0.2$ is an efficiency factor characterizing the gravitational collapse upon reentry of the metric fluctuations responsible for the PBH formation, and H_N is the rate of expansion during inflation at the time of horizon exit, while N is the number of e-folds when the fluctuation exits during inflation. For fluctuations produced during the near-inflection point, this rate is given (e.g. for the model parameters $a = 3/2$, $b = 1$ and $x_0 = 1$) by

$$H_N = 1.33 \times 10^{-6} M_P. \quad (4.4)$$

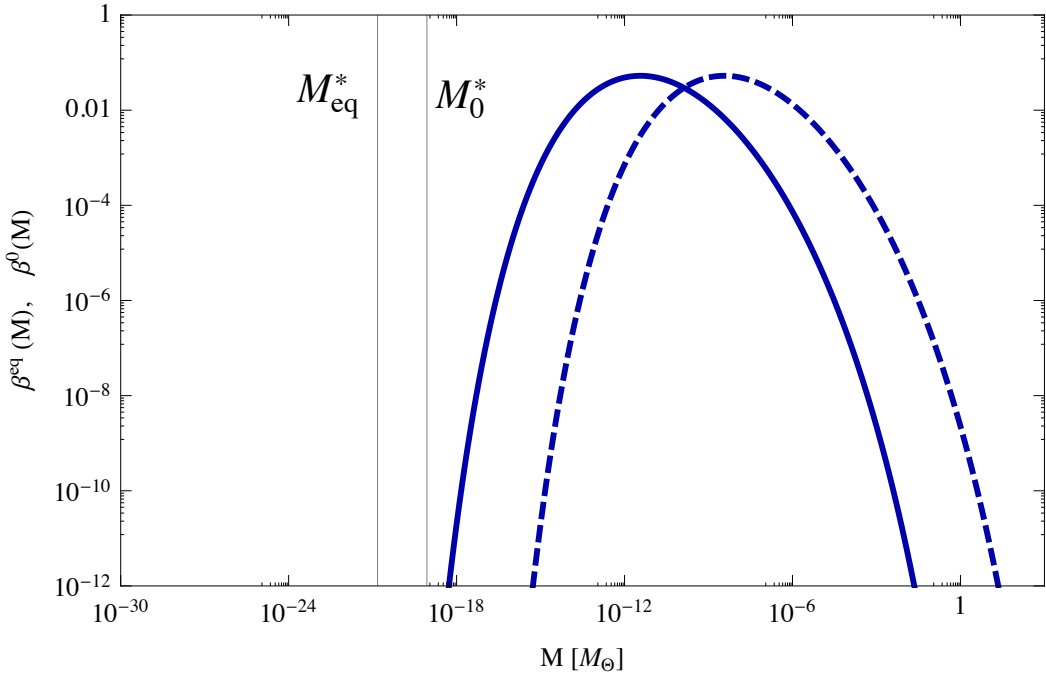


Figure 7. The mass distribution of PBH at equality (continuous line) and today (dashed line), for model parameters: $a = 3/2$, $b = 1$, $\zeta_c = 0.086$, $\Delta N = 45$ and $\beta = 5 \times 10^{-5}$. The vertical lines correspond to M_{eq}^* , the lower mass of PBH that survived until matter radiation equality, and M_0^* the mass of those that survived until today.

Putting all together, one finds the mass of PBHs, in solar mass units, as a function of N ,

$$M_{\text{PBH}} = M_\odot e^{2(N-36.48)}. \quad (4.5)$$

4.1 PBH evaporation in broad mass distributions

When PBH form, their whole distribution cover a wide range of masses, some of which will evaporate immediately, much before nucleosynthesis, while others will remain until matter radiation equality and recombination, and yet another group of more massive PBH will remain today to form the Dark Matter.

The evaporation via Hawking radiation is a runaway process that lasts a fraction of a second for small BHs, but can take much more than the age of the universe for massive ones,

$$\tau_{\text{ev}} = 5120 \pi \sqrt{\frac{\hbar G}{c^5}} \left(\frac{M_{\text{PBH}}}{M_P} \right)^3 = 2.1 \times 10^{67} \text{ yr} \left(\frac{M_{\text{PBH}}}{M_\odot} \right)^3 = 13.8 \text{ Gyr} e^{6(N-14.537)}. \quad (4.6)$$

Their relative abundance today will depend on their initial mass (4.5) and their relative abundance (4.2). Those that do not evaporate during the radiation era will come to dominate the density of the universe at matter-radiation equality. Their abundance will grow relative to that of radiation since formation to equality by a factor [13]

$$\beta^{\text{eq}}(M) = \frac{a_{\text{eq}}}{a(t_M)} \beta^{\text{form}}(M), \quad (4.7)$$

and their contribution to the matter content of the universe at equality is

$$\Omega_{\text{PBH}}^{\text{eq}} = \int_{M^*}^{M_{\text{eq}}} \frac{dM}{M} \beta^{\text{eq}}(M) = \int_{12.51}^{38} 2 dN \frac{a_{\text{eq}}}{a_0} e^{65-N} \beta^{\text{form}}(N), \quad (4.8)$$

where $M^* \simeq 3 \times 10^{12}$ g is the lower mass limit of those PBH that have survived until equality without evaporating. The final number, $\Omega_{\text{PBH}}^{\text{eq}} = 0.42$, corresponds to the case where these PBH constitute all of the DM today (the rest of matter at equality, $\Omega_B^{\text{eq}} = 0.08$, corresponds to baryons). For the parameters of the model, $a = 3/2$, $b = 1$, $\Delta N = 45$ and $\beta = 5 \times 10^{-5}$, we have found that $\zeta_c = 0.086$ gives rise to $\Omega_{\text{PBH}}^{\text{eq}} = 0.42$ at equality. We have plotted in Fig. 7 the mass distribution of PBH today assuming a factor 10^3 increase in mass due to merging. The effect of gas accretion is not taken into account in this figure, and is expected to significantly raise the tail of the distribution for larger masses.

5 Discussion and Conclusions

We have shown that it is possible to construct single-field models of inflation that satisfy all the constraints on large scales (from the CMB to compact minihalos LSS) and at the same time provide a mechanism for generating the observed Dark Matter in the form of PBH. The main advantage of single-field models is the economy of means. What multi-field models like hybrid inflation or axion inflation generate with new couplings, can be done here with a plateau feature in the single-scalar-field potential. We have succeeded in producing a peak in the primordial curvature power spectrum with just two parameters that govern the width and height of the inflationary plateau. While most models of inflation are only probed at CMB and LSS scales, i.e. approximately 60 to 50 e-folds before the end of inflation, the range of values of the field relevant for PBH production and the CMB covers the whole range, from 60 to the end of inflation. What is surprising is that generating a peak in the spectrum did not require any special fine-tuning of parameters for the amplitude of CMB fluctuations; actually, for our choice of parameters, the inflaton self-coupling λ turns out to be of order 10^{-7} , and the inflaton mass is of order the GUT scale.

The fact that quantum fluctuations of the inflaton field can backreact on space-time and form classical inhomogeneities, giving rise to CMB anisotropies and big structures like galaxies and clusters, is a fascinating property of Quantum Field Theory in curved space, and one of the great successes of inflation. What is even more surprising is that a local feature in the inflaton dynamics can give rise to large amplitude fluctuations in the spatial curvature, which collapse to form black holes upon reentry during the radiation era, and that these PBH may constitute today the bulk of the matter in the universe. In this new scenario, Dark Matter is no longer a particle produced after inflation, whose interactions must be deduced from high energy particle physics experiments, but an object formed by the gravitational collapse of relativistic particles in the early universe when subject to high curvature gradients, themselves produced by quantum fluctuations of a field and stretched to cosmological scales by inflation.

This opens a new window into the Early Universe. Cosmological observations of PBH as the main component of dark matter in the present universe, mainly the characterization of their mass distribution, may give us information about the inflaton dynamics just a few tens of e-folds before the end of inflation. Moreover, this new paradigm has many consequences [13]. For instance, this scenario could explain the missing satellite problem of N-body simulations, and makes specific predictions for the existence of massive black holes at the center of *all* large

scale structures, from dwarf spheroidals to massive galaxies [46]. The hierarchical merger tree scenario of structure formation then predicts that dark matter halos are composed of an intermediate mass black hole at their center, plus a smooth component of lighter PBH orbiting the halos. These building blocks will then merge to form larger structures like galaxies and clusters of galaxies.

What characterizes this scenario of inflation with broad peaks in $P_{\mathcal{R}}(k)$ [13, 14] is the small scale structure they predict. Rather than waiting for 5σ peaks in a Gaussian low-amplitude spectrum to gravitationally collapse to form the first stars after recombination, here the large-amplitude peaks in the primordial spectrum are enough to produce the PBH that will act as seeds on which gas will accrete and form galaxies. This scenario is thus responsible for reionization at high redshifts and early structure formation, which may explain why we observe fully formed structures like galaxies and QSO so far back in time, very soon after photon decoupling, and why there are strong spatial correlations between the cosmic near IR background and the soft-X-ray background fluctuations [17].

Furthermore, in this single-field model the economy of parameters imply that high curvature peaks cover a broad range of scales, and thus give rise to PBH with a large range of masses. The evaporation of these light PBH, between their time of formation and matter-radiation equality, is a new feature of this model. The rest of massive PBH will constitute the DM. Note that the large metric (curvature) perturbations remain there on small scales even if the PBH that formed by them upon reentry have evaporated today. Those large fluctuations will grow since equality and recombination due to the gravitational collapse of gas and PBH as DM around them, and will generate structures on extremely small scales, thus acting as early seeds for galaxies.

Fortunately, with the advent of Gravitational Wave Astronomy we have a completely new way of investigating both the late and the early universe. The gravitational wave background from the time of formation of PBH will leave signatures on PTA and LISA scales, while the inspiralling of PBHs to form more massive ones can be seen as chirps in both LISA and AdvLIGO-VIRGO. The stochastic background from these inspirals will cover the whole range from nHz to kHz, and in the not so far future, LISA and the Einstein Telescope will be able to detect such a background and hopefully determine the shape of the mass distribution.

We have entered a new era, with a new scenario of structure formation based on compact BH as the dominant component of Dark Matter, and new detectors in the form of laser interferometers, both on the ground and in space. We will be able to use these new tools to explore the formation of PBH in the early universe and connect these with the dynamics of inflation at energy scales close to the scale of quantum gravity, where present particle physics accelerators cannot reach.

Acknowledgements:

We thank Andrei Linde, Sebastien Clesse and Yashar Akrami for useful comments and discussions. We thank the hospitality of the Lorentz Institute in Leiden during the THCOS@LN meeting and specially Ana Achucarro for her generosity. This work is supported by the Research Project of the Spanish MINECO, FPA2015-68048-C3-3-P, and the Centro de Excelencia Severo Ochoa Program SEV-2012-0249.

References

- [1] P. J. E. Peebles, “How the Nonbaryonic Dark Matter Theory Grew,” arXiv:1701.05837 [astro-ph.CO].
- [2] L. Hui, J. P. Ostriker, S. Tremaine and E. Witten, “On the hypothesis that cosmological dark matter is composed of ultra-light bosons,” arXiv:1610.08297 [astro-ph.CO].
- [3] B. Carr, F. Kuhnel and M. Sandstad, Phys. Rev. D **94**, no. 8, 083504 (2016) [arXiv:1607.06077 [astro-ph.CO]].
- [4] M. Y. Khlopov, Res. Astron. Astrophys. **10**, 495 (2010), [arXiv:0801.0116 [astro-ph]].
- [5] G. F. Chapline, “Cosmological effects of primordial black holes,” Nature **253**, 251 (1975)
- [6] B. J. Carr and S. W. Hawking, Mon. Not. Roy. Astron. Soc. **168**, 399 (1974).
- [7] A. Dolgov and J. Silk, Phys. Rev. D **47**, 4244 (1993).
- [8] K. Jedamzik, Phys. Rev. D **55**, 5871 (1997) [astro-ph/9605152].
- [9] Y. Aoki, G. Endrodi, Z. Fodor, S. D. Katz and K. K. Szabo, Nature **443**, 675 (2006), [hep-lat/0611014].
- [10] J. García-Bellido, A. D. Linde and D. Wands, Phys. Rev. D **54**, 6040 (1996) [astro-ph/9605094].
- [11] J. Yokoyama, Astron. Astrophys. **318**, 673 (1997) [astro-ph/9509027].
- [12] T. Nakamura, M. Sasaki, T. Tanaka and K. S. Thorne, Astrophys. J. **487**, L139 (1997) [astro-ph/9708060].
- [13] S. Clesse and J. García-Bellido, Phys. Rev. D **92**, no. 2, 023524 (2015) [arXiv:1501.07565 [astro-ph.CO]].
- [14] J. García-Bellido, M. Peloso and C. Unal, JCAP **1612**, no. 12, 031 (2016), [arXiv:1610.03763 [astro-ph.CO]].
- [15] F. Vito *et al.* [Chandra Collaboration], Mon. Not. Roy. Astron. Soc. **463**, 348 (2016), [arXiv:1608.02614 [astro-ph.GA]],
- [16] B. Luo *et al.* [Chandra Collaboration], Astrophys. J. Suppl. **228**, no. 1, 2 (2017), [arXiv:1611.03501 [astro-ph.GA]].
- [17] A. Kashlinsky, Astrophys. J. **823**, no. 2, L25 (2016), [arXiv:1605.04023 [astro-ph.CO]].
- [18] J. R. Chisholm, Phys. Rev. D **73**, 083504 (2006), [astro-ph/0509141].
- [19] J. R. Chisholm, Phys. Rev. D **84**, 124031 (2011), [arXiv:1110.4402 [astro-ph.CO]].
- [20] B. P. Abbott *et al.* [LIGO Scientific and Virgo Collaborations], Phys. Rev. Lett. **116**, no. 6, 061102 (2016), [arXiv:1602.03837 [gr-qc]].
- [21] S. Bird, I. Cholis, J. B. Muñoz, Y. Ali-Haïmoud, M. Kamionkowski, E. D. Kovetz, A. Raccanelli and A. G. Riess, Phys. Rev. Lett. **116**, no. 20, 201301 (2016), [arXiv:1603.00464 [astro-ph.CO]].
- [22] S. Clesse and J. García-Bellido, Phys. Dark Univ. **10**, 002 (2016), [arXiv:1603.05234 [astro-ph.CO]].
- [23] M. Sasaki, T. Suyama, T. Tanaka and S. Yokoyama, Phys. Rev. Lett. **117**, no. 6, 061101 (2016), [arXiv:1603.08338 [astro-ph.CO]].
- [24] M. Kawasaki, A. Kusenko, Y. Tada and T. T. Yanagida, Phys. Rev. D **94**, no. 8, 083523 (2016), [arXiv:1606.07631 [astro-ph.CO]].
- [25] T. Nakama, T. Suyama and J. Yokoyama, Phys. Rev. D **94**, no. 10, 103522 (2016), [arXiv:1609.02245 [gr-qc]].

[26] S. Blinnikov, A. Dolgov, N. K. Porayko and K. Postnov, JCAP **1611**, no. 11, 036 (2016), [arXiv:1611.00541 [astro-ph.HE]].

[27] E. Erfani, JCAP **1604**, no. 04, 020 (2016), [arXiv:1511.08470 [astro-ph.CO]].

[28] H. Deng, J. Garriga and A. Vilenkin, “Primordial black hole and wormhole formation by domain walls,” arXiv:1612.03753 [gr-qc].

[29] A. Raccanelli, E. D. Kovetz, S. Bird, I. Cholis and J. B. Munoz, Phys. Rev. D **94**, no. 2, 023516 (2016), [arXiv:1605.01405 [astro-ph.CO]].

[30] K. Belczynski *et al.*, Astron. Astrophys. **594**, A97 (2016), [arXiv:1607.03116 [astro-ph.HE]].

[31] B. P. Abbott *et al.* [LIGO Scientific and Virgo Collaborations], Phys. Rev. Lett. **116**, no. 24, 241103 (2016), [arXiv:1606.04855 [gr-qc]].

[32] B. P. Abbott *et al.* [LIGO Scientific and Virgo Collaborations], Phys. Rev. X **6**, no. 4, 041015 (2016), [arXiv:1606.04856 [gr-qc]].

[33] B. P. Abbott *et al.* [LIGO Scientific and Virgo Collaborations], Annalen Phys. **529**, 1600209 (2016), [arXiv:1608.01940 [gr-qc]].

[34] B. P. Abbott *et al.* [LIGO Scientific and Virgo Collaborations], Phys. Rev. Lett. **116**, no. 13, 131102 (2016), [arXiv:1602.03847 [gr-qc]].

[35] V. Mandic, S. Bird and I. Cholis, Phys. Rev. Lett. **117**, no. 20, 201102 (2016), [arXiv:1608.06699 [astro-ph.CO]].

[36] S. Clesse and J. García-Bellido, “Detecting the gravitational wave background from primordial black hole dark matter,” arXiv:1610.08479 [astro-ph.CO].

[37] N. Bartolo *et al.*, JCAP **1612**, no. 12, 026 (2016), [arXiv:1610.06481 [astro-ph.CO]].

[38] R. Allahverdi, K. Enqvist, J. García-Bellido and A. Mazumdar, Phys. Rev. Lett. **97**, 191304 (2006), [hep-ph/0605035].

[39] R. Allahverdi, K. Enqvist, J. García-Bellido, A. Jokinen and A. Mazumdar, JCAP **0706**, 019 (2007), [hep-ph/0610134].

[40] A. D. Linde and A. Westphal, JCAP **0803**, 005 (2008), [arXiv:0712.1610 [hep-th]].

[41] S. Hotchkiss, A. Mazumdar and S. Nadathur, JCAP **1106**, 002 (2011), [arXiv:1101.6046 [astro-ph.CO]].

[42] J. García-Bellido and D. Roest, Phys. Rev. D **89**, no. 10, 103527 (2014), [arXiv:1402.2059 [astro-ph.CO]].

[43] T. Bringmann, P. Scott and Y. Akrami, Phys. Rev. D **85**, 125027 (2012), [arXiv:1110.2484 [astro-ph.CO]].

[44] P. A. R. Ade *et al.* [Planck Collaboration], Astron. Astrophys. **594**, A20 (2016), [arXiv:1502.02114 [astro-ph.CO]].

[45] P. A. R. Ade *et al.* [Planck Collaboration], Astron. Astrophys. **594**, A13 (2016), [arXiv:1502.01589 [astro-ph.CO]].

[46] T. S. Li *et al.* [DES Collaboration], “Farthest Neighbor: The Distant Milky Way Satellite Eridanus II,” [arXiv:1611.05052 [astro-ph.GA]].